



HAL
open science

Influence of ablation-related processes in the build-up of simulated Northern Hemisphere ice sheets during the last glacial cycle

S. Charbit, C. Dumas, M. Kageyama, Didier M. Roche, C. Ritz

► To cite this version:

S. Charbit, C. Dumas, M. Kageyama, Didier M. Roche, C. Ritz. Influence of ablation-related processes in the build-up of simulated Northern Hemisphere ice sheets during the last glacial cycle. *The Cryosphere*, 2013, 7 (2), pp.681-698. 10.5194/tc-7-681-2013 . hal-02922666

HAL Id: hal-02922666

<https://hal.science/hal-02922666>

Submitted on 8 Sep 2020

HAL is a multi-disciplinary open access archive for the deposit and dissemination of scientific research documents, whether they are published or not. The documents may come from teaching and research institutions in France or abroad, or from public or private research centers.

L'archive ouverte pluridisciplinaire **HAL**, est destinée au dépôt et à la diffusion de documents scientifiques de niveau recherche, publiés ou non, émanant des établissements d'enseignement et de recherche français ou étrangers, des laboratoires publics ou privés.



Influence of ablation-related processes in the build-up of simulated Northern Hemisphere ice sheets during the last glacial cycle

S. Charbit¹, C. Dumas¹, M. Kageyama¹, D. M. Roche¹, and C. Ritz²

¹IPSL/Laboratoire des sciences du climat et de l'environnement, UMR CEA-CNRS-UVSQ 8212, CE Saclay, Orme des Merisiers, Bât. 701, 91191 Gif-sur-Yvette cedex, France

²UJF – Grenoble 1/CNRS, Laboratoire de glaciologie et de géophysique de l'environnement, UMR 5183, Grenoble, 38041, France

Correspondence to: S. Charbit (sylvie.charbit@lsce.ipsl.fr)

Received: 4 October 2012 – Published in The Cryosphere Discuss.: 28 November 2012

Revised: 7 March 2013 – Accepted: 13 March 2013 – Published: 18 April 2013

Abstract. Since the original formulation of the positive-degree-day (PDD) method, different PDD calibrations have been proposed in the literature in response to the increasing number of observations. Although these formulations generally provide a satisfactory description of the present-day Greenland geometry, they have not all been tested for paleo ice sheets. Using the climate-ice sheet model CLIMBER-GRISLI coupled with different PDD models, we evaluate how the parameterisation of the ablation may affect the evolution of Northern Hemisphere ice sheets in the transient simulations of the last glacial cycle. Results from fully coupled simulations are compared to time-slice experiments carried out at different key periods of the last glacial period. We find large differences in the simulated ice sheets according to the chosen PDD model. These differences occur as soon as the onset of glaciation, therefore affecting the subsequent evolution of the ice system. To further investigate how the PDD method controls this evolution, special attention is given to the role of each PDD parameter. We show that glacial inception is critically dependent on the representation of the impact of the temperature variability from the daily to the inter-annual time scale, whose effect is modulated by the refreezing scheme. Finally, an additional set of sensitivity experiments has been carried out to assess the relative importance of melt processes with respect to initial ice sheet configuration in the construction and the evolution of past Northern Hemisphere ice sheets. Our analysis reveals that the impacts of the initial ice sheet condition may range from quite negligible to explaining about half of the LGM ice volume depending on the representation of stochastic tempera-

ture variations which remain the main driver of the evolution of the ice system. The main findings of this paper underline the need for conducting studies with high resolution climate models coupled to detailed snow models to better constrain the temporal and spatial variations of the PDD parameters. The development of such approaches could improve the calibration of the PDD formulation which is still widely used in climate-ice sheet studies.

1 Introduction

Simulating the surface mass balance of polar ice sheets correctly is crucial to better understand climate and ice sheet feedbacks at decadal to multi-millennial time scales and to better predict the evolution of present-day ice sheets in the coming decades. The surface mass balance is defined as the sum of the surface accumulation and the surface ablation. The ablation of snow and ice is closely linked to the energy balance at the surface of the ice sheets. Several processes strongly influence the energy exchanges at the surface-atmosphere interface. As an example, in addition to solar radiation and cloud optical properties that directly influence the near-surface air temperatures (Key et al., 2001; van den Broecke et al., 2008), katabatic winds may have a huge impact on turbulent heat transfer (Oerlemans and Hoogendoorn, 1989; van den Broecke et al., 1994). The energy balance is also a function of surface characteristics and snow properties, such as roughness length, snow temperature, snow density, shape and size of grains, water content

in the snowpack and snow and ice albedo (Brun et al., 1989, 1992). This underlines the need for having an accurate representation of snow and atmospheric processes to properly compute the energy balance at the surface of the ice sheets (Gallée and Duynkerke, 1997). However, such a representation requires a detailed snow model and a climate model having a resolution equivalent to or finer than the spatial scale needed to accurately resolve the ablation zone (i.e., ~ 10 km; van den Broecke et al., 2008). The horizontal resolution of current climate models is far beyond this limit and, owing to their high computational cost, the use of regional atmospheric models (Lefebvre et al., 2005; Ettema et al., 2009; Fettweis, 2007, 2011, 2013) is impossible for integrations spanning over centuries or millennia.

An alternative approach consists in using the empirical positive-degree-day (PDD) method that relates positive air temperatures to ablation. This concept was first applied to alpine glaciers in the late 19th century (Finsterwalder and Schunk, 1887), but the early mathematical formulation of the PDD method was proposed by Braithwaite (1984). Observations recorded in ice-margin locations in Western Greenland (Braithwaite and Olesen, 1989) later confirmed a strong correlation between ablation and mean surface air temperature. Relying on this work, Reeh (1991) modified the original PDD formulation of Braithwaite (1984) to provide a parameterisation of the ablation that can be used over the whole Greenland ice sheet: the amount of positive-degree-days is converted in melt rates of snow and ice through degree-day factors (DDF) in combination with a meltwater retention/refreezing scheme and the fluctuations of temperature around the daily mean are accounted for (see Sect. 2). Due to its simplicity, this modified PDD formulation has been widely used in mass balance computations and has been favourably compared to observations (Huybrechts et al., 1991; Ritz et al., 1997, 2001). It has also been widely used in paleo-climatic contexts to study the ice-sheet response to a given climatic evolution (Abe-Ouchi et al., 2007; Charbit et al., 2007, 2002; Graverson et al., 2010; Greve, 2005; Stone et al., 2010; Zweck and Huybrechts, 2005) or to study the climate-ice sheet feedbacks (Bonelli et al., 2009; Charbit et al., 2005; Kageyama et al., 2004; Philippon et al., 2006; Swingedouw et al., 2008; Vizcaino et al., 2008).

However, according to a compilation of measurements carried out over several European and Greenland glaciers, it appears that DDF values largely differ from one location to the other (Braithwaite and Zhang, 2000; Hock, 2003) making questionable the use of one single DDF value to compute snow melt rate and another single one for ice. As a consequence, numerous attempts to improve the formulation of Reeh (1991) have then been proposed. These attempts include the representation of the refreezing process (Pfeffer et al., 1991; Janssens and Huybrechts, 2000), the calibration of new degree-day factors (Braithwaite, 1995; Tarasov and Peltier, 2002), and more recently a new parameterisation of the standard distribution of surface air temperatures (Fausto

et al., 2009). The net consequence is that a growing number of PDD formulations appears in the literature. Although these formulations are calibrated against small-scale observations of present-day Greenland based on different sampling data, they have usually been revealed successful for the large-scale representation of the ice sheet geometry despite some regional deficiencies. However, with the exception of Reijmer et al. (2012) who compared different refreezing schemes with outputs from a regional atmospheric climate model, no PDD inter-comparison has been undertaken so far. It is, therefore, difficult to evaluate the performance and the efficiency of each PDD parameterisation for present-day ice sheets. Moreover, as recently outlined by van de Berg et al. (2011), the calibration of the PDD models against present-day Greenland is not necessarily valuable in paleo-climatic contexts for which insolation conditions, seasonal and spatial climatic variability, snow metamorphism and locations and shapes of ice sheets were rather different from those observed for modern days. The problem becomes even more complex for studies carried out with a coupled climate-ice sheet model where the climate-ice sheet feedbacks may amplify or mitigate the effect of temperature forcing. Therefore, there is a crucial need for further refinement of temperature-melt models used in different climatic contexts.

In this study, we test several PDD formulations in the simulation of the last glacial cycle. Here, the PDD approach is used as a tool to evaluate the relative importance of both ice-sheet initial configuration and ablation-related processes in the build-up of Northern Hemisphere ice sheets throughout this period. To achieve this goal, we first test the sensitivity of the surface mass balance of Northern Hemisphere ice sheets to different PDD formulations and we evaluate the impact of each PDD parameter in this response. Secondly, through a set of sensitivity experiments, we investigate the relative impact of the ice-sheet feedbacks onto the climate (i.e., through a change of initial ice-sheet geometry) and, therefore, on the evolution of the ice system with respect to the way the ablation is computed.

2 PDD formulations

2.1 The standard PDD formulation

The PDD method was first proposed by Braithwaite (1984) and relies on the assumption that the annual surface melting is proportional to the sum over one year of the excess of temperature above the melting point, also called the positive degree-day sum. It was suggested that the number of positive degree-days could be calculated from the normal probability distribution around the mean monthly temperatures (Braithwaite, 1984). Reeh (1991) modified this formulation by computing the positive degree-day sum from the mean daily temperatures and the variations around the daily mean.

This new formulation (hereafter referred to as the standard formulation) has been since widely used in ice-sheet models and is expressed as:

$$\text{PDD} = \frac{1}{\sigma\sqrt{2\pi}} \int_{1\text{yr}} dt \int_0^{T_d+2.5\sigma} T \cdot \exp\left[-\frac{(T - T_d(t))^2}{2\sigma^2}\right] dT \quad (1)$$

where T_d represents the daily temperature, and σ the standard deviation of the temperature distribution. The average annual temperature cycle is assumed to follow a cosine function with amplitude given by the difference between mean summer (T_{jja}) and mean annual (T_{ann}) air temperatures and a period A of 1 yr. Therefore, the mean daily temperature is expressed as:

$$T_d(t) = T_{\text{ann}}(t) + (T_{\text{jja}} - T_{\text{ann}}) \cos \frac{2\pi t}{A} \quad (2)$$

As previously stated, it is generally assumed that σ represents the deviations from the mean daily temperature. These random fluctuations are important because they may cause the occurrence of positive temperatures (and, hence, surface melting) even though the mean daily temperature is below the freezing point. In the standard formulation of Reeh (1991), σ is set to 5 °C. In practice, especially for uses in paleo-climatic contexts, this parameter accounts for the overall stochastic variations of temperatures such as those occurring at the inter-annual time scale. However, there is no real reason to assume $\sigma = 5$ °C (Braithwaite, 1984).

Observations at West Greenland locations revealed a high correlation between air temperatures and melt rates (Braithwaite and Olesen, 1989). Melting of snow and ice is therefore linearly related to the number of PDD through the degree-day factors C_{snow} and C_{ice} for snow and ice, respectively. To account for albedo difference between snow and ice, C_{snow} and C_{ice} have different values. Following observations of Braithwaite and Olesen (1989) and Braithwaite (1995) the standard C_{snow} and C_{ice} were fixed to 3 mm w.e. °C⁻¹ d⁻¹ and 8 mm w.e. °C⁻¹ d⁻¹, respectively.

Meltwater produced at the surface may refreeze or may percolate in the snowpack and forms superimposed ice. In the standard PDD formulation (Reeh, 1991), the maximum amount of superimposed ice (P_{max}) cannot exceed 60 % of the amount of water coming from melting of the annual snowfall. This value corresponds to the ratio of the annual surface melt to the annual accumulation at the runoff limit (Braithwaite and Thomsen, 1989), defined as the lower boundary of the zone where all meltwater is refrozen. This ratio is closely related to refreezing since it describes firn-density variations and since the density in the near-surface firn layer is mainly controlled by the formation of ice layers due to refreezing (Braithwaite, 1994). Further measurements of firn density made in the lower accumulation area of the Greenland ice sheet led Braithwaite (1994) to refine this ratio to 0.58. With a more sophisticated refreezing model, Pfeffer

et al. (1991) found a slightly larger value of 0.7, reduced to 0.62 if numerical density values of snow and ice equal those of Braithwaite (1994). Therefore, although the P_{max} value seems to have been chosen somewhat arbitrarily, it is more physically based than it looks and leads to estimates of firn warming resulting from latent heat release after meltwater refreezing in reasonable agreement with observations (Reeh, 1991).

Following the PDD model formulated by Reeh (1991), the melting of snow and ice follows a three-step process: (1) Snow is first melted at the rate C_{snow} . Meltwater percolates into the snowpack and refreezes at depth. Runoff occurs when the amount of superimposed ice exceeds 60 % of the yearly snowfall. (2) Superimposed ice is then melted. (3) Glacier ice is melted. This process can be interrupted at any of the stages 1–3, depending on the available energy, that is on the amount of PDD.

2.2 Dependency of degree-day factors on temperature

Since the standard PDD formulation proposed by Reeh (1991), new observational data have become available, such as the GIMEX (Oerlemans and Vugts, 1993) and the Camp IV (Ambach, 1988) experimental campaigns launched to improve the understanding of processes governing the ice-sheet mass balance. These experiments revealed a strong dependency of DDF (especially for ice material) with temperature, and values of C_{ice} as high as ~18–20 mm w.e. °C⁻¹ d⁻¹ were found at high elevations and in northern regions of Greenland. Relying on energy balance modelling, Braithwaite (1995) also found evidence of the dependency of DDF with temperature, with large values at lower temperatures. A compilation of positive degree-day factors at various locations can be found in Braithwaite and Zhang (2000) and Hock (2003). This wide range of DDF values has been attributed to temporal and spatial variations of energy balance characteristics reviewed in Hock (2003) and has been later confirmed by modelling studies carried out by Lefebvre et al. (2002) for the 1991 melt season. These findings led several authors to refine the Reeh's PDD formulation. As an example, Greve (2000) introduced a latitudinal dependency of ice melt factors. Tarasov and Peltier (2002) added a dependency of DDF on mean summer temperature (see Sect. 3). Following Tarasov and Peltier (2002), Greve (2005) combined both latitudinal and temperature dependencies of DDF and derived a similar relation between DDF and the mean July near-surface air temperature. This approach has also further been used by Fausto et al. (2009).

2.3 Revised treatment of meltwater retention

A critical issue in ice-sheet mass balance studies is the percolation of surface meltwater which is then retained at depth and refreezes as superimposed ice. This process delays and reduces the runoff and may induce large uncertainties in the

Table 1. Standard fully coupled CLIMBER-GRISLI simulations.

Forcings	Insolation CO ₂ Sea level	Laskar et al. (2004) Petit et al. (1999) Waelbroeck et al. (2002)	
Initial Conditions	PDD Models	References	Run ID
126 kyr climate	RH91	Reeh (1991)	1
Present-day Greenland topography	TP02	Tarasov and Peltier (2002)	2
	FST09	Adapted from Fausto et al. (2009)	3

estimation of glacier mass balance if not accounted for. A common way to deal with this retention process is to define the “potential retention fraction” (Pr) which represents the maximum of liquid water that can be refrozen before runoff occurs. The importance of this process has broadly been addressed in the literature through a variety of different retention models (Fausto et al., 2009; Huybrechts and de Wolde, 1999; Janssens and Huybrechts, 2000; Pfeffer et al., 1991; Tarasov and Peltier, 2002). The lower bound model sets Pr to zero (i.e., no retention takes place). The approach followed by Reeh (1991) is one of the simplest: the potential retention fraction is given by a constant and spatially uniform fraction of the snowmelt ($P_{\max} = 0.6$) and is defined by:

$$Pr = P_{\max} \times Acc \quad (3)$$

where “Acc” represents the annual snow accumulation.

Huybrechts and de Wolde (1999) used a simple thermodynamic parameterisation of the refreezing process in which the maximum amount of refrozen ice is related to the amount of latent heat release needed to remove the cold content of snow of the upper ice sheet layers. When the maximum amount of superimposed ice is reached, any additional production of water coming from snowmelt or rainfall will escape as runoff. Janssens and Huybrechts (2000) went a step further and added to the formulation of Huybrechts and de Wolde (1999) a term accounting for refreezing of capillary water filling the pore space in the snowpack. More recently Fausto et al. (2009) considered a retention/refreezing model, based on the formulation of Janssens and Huybrechts (2000), but with snow density varying as a function of time. This allows the densification effects to be accounted for (Zwally and Li, 2002). These effects may affect runoff through a reduction of both the thermal active layer thickness and the volume of the pore storage for meltwater within the annual snow layer, thereby decreasing the ability of the snowpack to retain water.

2.4 PDD formulations adopted in the present study

Our approach aims at comparing the sensitivity of simulated ice sheets to three distinct PDD models dealing with PDD parameters (i.e., DDF factors, retention/refreezing scheme and standard deviation of temperatures) in a different way. The

first model is exactly the same as the one proposed by Reeh (1991), referred hereafter to as to RH91 (see Sect. 2.1 and Table 1). The second one is that used by Tarasov and Peltier (2002), and the third one is inspired by the study of Fausto et al. (2009). In the following, these models are respectively referred to as TP02 and FST09.

2.4.1 TP02 Model

The standard deviation of temperature chosen in TP02 is $\sigma = 5.2^\circ\text{C}$, quite similar to that of RH91 ($\sigma = 5.0^\circ\text{C}$). Snow and ice ablation factors (C_{snow} and C_{ice}) depend on mean summer temperature (T_{jja}):

$$C_{\text{ice}} = \begin{cases} 17.22 & \text{if } T_{\text{jja}} \leq -1^\circ\text{C} \\ 0.0067 \times (10 - T_{\text{jja}})^3 + 8.3 & \text{if } -1^\circ\text{C} < T_{\text{jja}} < 10^\circ\text{C} \\ 8.3 & \text{if } 10^\circ\text{C} \leq T_{\text{jja}} \end{cases} \quad (4)$$

$$C_{\text{snow}} = \begin{cases} 2.65 & \text{if } T_{\text{jja}} \leq -1^\circ\text{C} \\ 0.15 \times T_{\text{jja}} + 2.8 & \text{if } -1^\circ\text{C} < T_{\text{jja}} < 10^\circ\text{C} \\ 4.3 & \text{if } 10^\circ\text{C} \leq T_{\text{jja}} \end{cases} \quad (5)$$

C_{ice} and C_{snow} are given in $\text{mm ice-equivalent } ^\circ\text{C}^{-1} \text{d}^{-1}$. Although these formulations represent a step forward in the calculation of the ablation with the PDD approach, they do not account for the impact of changing surface conditions without changing climatic variables (Braithwaite, 1995).

The refreezing scheme is based on the same principles as the one given by Janssens and Huybrechts (2000). It represents the removal of the cold content of the thermally active layer by the release of latent heat accompanying the refreezing of meltwater. If enough water refreezes, the temperature of this layer may be raised to the melting point and runoff may occur (Pfeffer et al., 1991). Secondly, the refreezing scheme describes the saturation effect of the snow pore space, so that refreezing of capillary water may occur at the end of the melt season. The amount of superimposed ice (refrozen snow melt and frozen rain) for each year is given by:

$$\begin{aligned} & \min \left[P - A + M, (A - M) \times \left(\frac{\rho_e}{\rho_0} - 1 \right) - d \times \frac{c}{L} \times \min(T_{\text{ann}}, 0^\circ\text{C}) \right] \\ & \text{if } M < A \\ & \min \left[P - A + M, d \times \frac{c}{L} \times \min(T_{\text{ann}}, 0^\circ\text{C}) \right] \\ & \text{if } M > A \end{aligned} \quad (6)$$

$L = 3.35 \times 10^5 \text{ J kg}^{-1}$ and $c = 2115.3 + 7.79 \times T_{\text{ann}} \text{ J kg}^{-1} \text{ K}^{-1}$, with T_{ann} expressed in degrees Celsius, are respectively the latent heat of fusion and the specific heat capacity of the ice. Note that c comes from the original study of Ritz et al. (1997) and slightly differs from that used in Tarasov and Peltier (2002). However, this slight difference does not impact so much the results. T_{ann} is the mean annual temperature, P is the total precipitation, A is the annual snow accumulation and M is the yearly snow-melt. The quantities $\rho_0 = 300 \text{ kg m}^{-3}$ and $\rho_e = 960 \text{ kg m}^{-3}$ are respectively the densities of surface snow and water-saturated wet snow, and d represents the thickness of the thermal active layer. In Tarasov and Peltier (2002), as in the present study, d is set to 1 m, while in Janssens and Huybrechts (2000), the thermal active layer has a variable thickness given by the annual snow accumulation A .

2.4.2 FST09 Model

The temperature-dependent values of the C_{ice} parameter in the FST09 model are quite similar to those of the TP02 model:

$$C_{\text{ice}} = \begin{cases} 15.0 & \text{if } T_{\text{jja}} \leq -1^\circ\text{C} \\ 0.006 \times (10 - T_{\text{jja}})^3 + 7 & \text{if } -1^\circ\text{C} < T_{\text{jja}} < 10^\circ\text{C} \\ 7 & \text{if } 10^\circ\text{C} \leq T_{\text{jja}} \end{cases} \quad (7)$$

In contrast to TP02, the C_{snow} value is constant and is set to the standard value of $3 \text{ mm } ^\circ\text{C}^{-1} \text{ d}^{-1}$.

Using results based on their refreezing model accounting for densification effects, Fausto et al. (2009) demonstrated that the potential retention fraction is dependent on the elevation (see their Fig. 6), with almost no refreezing at low altitudes and 100 % meltwater moved to superimposed ice at high altitudes. We therefore used this result to derive a simple parameterisation of the maximum amount of superimposed ice expressed as a function of the altitude S of the ice sheet:

$$P_{\text{max}} = \begin{cases} 0 & \text{if } S \leq 800 \text{ m} \\ (S - 800) \times 8.33 \times 10^{-4} & \text{if } 800 \text{ m} < S < 2000 \text{ m} \\ 1 & \text{if } S \geq 2000 \text{ m} \end{cases} \quad (8)$$

The largest difference between FST09 and other models lies in the value of the standard deviation of temperature distribution. Values around $4.5\text{--}5.5^\circ\text{C}$ are commonly found in literature (Greve, 2005; Reeh, 1991; Ritz et al., 1997; Tarasov and Peltier, 1999, 2002). However, Fausto et al. (2009) argued that this parameter may vary considerably with geographic locations and altitude. Using observational data coming from automatic weather stations, they demonstrated that the altitudinal component dominated the amplitude of the standard deviation. In this study, we neglect the latitudinal and longitudinal dependencies and, following Fausto et al. (2009), we express σ as:

$$\sigma = 1.574 + 1.2224 \times 10^{-3} \times S \quad (9)$$

This formulation implies a larger variability of temperatures with increasing altitude. As reported by Fausto et al. (2009),

the surface temperature of a melting snow or ice surface is fixed to 0°C limiting the variability of the near-surface air temperature. When no melt occurs such as in winter or in high elevation areas, surface temperature variations are not limited by the melting point temperature, allowing a larger variability of the near-surface temperature

3 Models

The climate model used in this study, CLIMBER2.4, is a coupled atmosphere-ocean-vegetation model. It is a revised version of CLIMBER2.3 thoroughly described in Petoukhov et al. (2000).

The atmospheric and land surface modules have a coarse spatial resolution of $\sim 51^\circ$ in longitude and 10° in latitude. This atmospheric model follows a statistical-dynamical approach: prognostic variables are bi-dimensional (latitude, longitude) and the vertical profiles of temperature and humidity are reconstructed using the assumption of a universal vertical structure of the atmosphere. This model is designed to only resolve large-scale processes, but the effects of synoptic weather systems on heat and moisture transports are parameterised as diffusive terms. In the standard version of the model (Petoukhov et al., 2000), stationary waves are parameterised as a function of the difference between sea-level temperature and its zonal mean. In the present study, we removed this ad hoc parameterisation which was at the origin of a cold bias over Beringia.

The ocean is described by three latitude-depth ($2.5^\circ \times 20$ uneven vertical layers) basins (Atlantic, Indian, Pacific) including the Arctic and the Austral Oceans. The main difference between CLIMBER2.4 and CLIMBER2.3 relies on a different oceanic advection scheme, which is of second order type in the new version and less diffusive. The ocean module also includes a thermodynamic sea ice model which predicts the sea ice fraction and thickness for each grid cell with a simple treatment of diffusion and advection.

The dynamical terrestrial vegetation model, VECODE, provides the distribution of trees, grasses and deserts in response to climate forcing. Each of these three surface types may be or not covered by snow. The atmosphere and vegetation modules are linked through an atmosphere-surface interface scheme describing the land surface processes. This interface module considers six surface types: open ocean, sea ice, trees, grasses, deserts and glaciers, with the possibility for all of these surface types to coexist in one grid cell.

The main advantage of CLIMBER compared to many other Earth models of intermediate complexity (Claussen et al., 2002) is that it includes a full description of the hydrological cycle: evaporation, humidity transport and precipitation are explicitly computed. Therefore, it is fully appropriate to be coupled with an ice-sheet model. Bonelli et al. (2009), Calov et al. (2005a, b) and Ganopolski et al. (2010) used the same kind of approach to account for the impact of dust

deposition on snow and ice albedos. In the present study, we did not use the parameterisation of the impact of dust deposition. Our choice was motivated by the fact that it could have been difficult to discriminate the effect of each PDD parameter from the effect of dust deposition since both have likely been different at various stages of the last glacial cycle. This represents another difference between the model used in the present study and its previous versions.

The large scale ice-sheet model, GRISLI, was first designed to describe the Antarctic ice sheet (Ritz et al., 2001) and adapted later on for the Northern Hemisphere ice sheets (Peyaud et al., 2007). A comprehensive description of the model is provided in these studies. GRISLI is a 3-D thermo-mechanical ice-sheet model which simulates the evolution of the geometry of ice sheets in response to climate forcing. It takes the coupled behaviour of temperatures and velocities into account. The model deals with the inland ice flow following the zero-order shallow-ice approximation. It also simulates the dynamics of ice shelves and fast ice flow occurring in ice stream zones. The width of ice streams being not greater than a few kilometres, individual ice streams are not explicitly resolved since the model resolution is $40 \text{ km} \times 40 \text{ km}$. Instead, the large-scale characteristics of fast flowing regions are represented with the shallow-shelf approximation (MacAyeal, 1989) using criteria based upon effective pressure (i.e., balance between ice and water pressure) and hydraulic load.

The model relies on basic principles of mass, heat and momentum conservation. Evolution of ice-sheet geometry is a function of surface mass balance, velocity fields and bedrock altitude. The isostatic adjustment of bedrock in response to ice load is governed by the flow of the asthenosphere, with a characteristic time constant of 3000 yr, and by the rigidity of the lithosphere. The temperature field is computed both in the ice and in the bedrock by solving a time-dependent heat equation. Locations of ice shelves are defined using a flotation criterion that depends on the ice thickness and the depth of bedrock below sea level. Ice shelves are also characterised by fast ice flow and low surface slope. Ice velocity is therefore determined with the same set of equations used for ice streams, but with a basal drag coefficient set to zero, except in regions of pinning points where the basal drag is assumed to be 20 times lower than in ice streams areas. Calving is not explicitly simulated, but the position of the ice-shelf front is reached when ice thickness in ice-shelf areas is below 150 m (Peyaud et al., 2007). Since the flotation criterion is checked at each time step of the simulation, the position of the grounding line is always determined. The grounding line may advance or retreat as sea level changes, especially during periods of huge ice volume variations such as glacial-interglacial cycles.

To account for the difference of resolution between CLIMBER and GRISLI, a specific downscaling procedure has been developed. The climatic fields used to compute the surface mass balance onto the GRISLI grid are the mean

annual and summer surface air temperatures and the annual snowfall. The surface mass balance is defined as the sum of the surface accumulation and the surface ablation. Ablation is computed using the PDD approach. For each CLIMBER grid box and each surface type, the temperature is computed on 5 vertical levels (between 0 and 4000 m) by using the surface air temperature and the free atmospheric lapse rate computed by the model. This procedure is similar to the one used by Bonelli et al. (2009), except that we do not take into account the effect of temperature inversion. The vertical precipitation profile is computed as a function of humidity depletion with temperatures obtained through the above mentioned procedure. For temperature fields, these calculations are performed for each CLIMBER surface types and averaged over the three GRISLI surface types (i.e., land ice, ice-free land, ocean). The mean annual and summer surface air temperatures as well as the annual snowfall are then trilinearly interpolated on the GRISLI grid. This procedure has been applied for both forced and coupled runs. In the coupled mode, any change in ice sheet geometry impacts the simulated climate: GRISLI computes the fraction of ocean, land ice and ice-free land as well as the altitude of continents which are given back to CLIMBER as new boundary conditions. The freshwater fluxes from ice melting are released to the CLIMBER oceans and are distributed according to a runoff mask based on the present-day topography. In the present version of the coupled model, the basal melt rate under the ice shelves is prescribed to fixed values which depend on the oceanic region.

Four series of simulations have been carried out to test the sensitivity of the simulated ice sheets to the PDD model (and thus to the PDD parameters) and to investigate the relative importance of ablation-related processes in the build-up of Northern Hemisphere ice sheets through the last glacial cycle with respect to initial ice-sheet geometry. The experimental set up of these simulations is described in Sects. 4 and 5 and summarised in Tables 1 to 4.

4 General results

4.1 Coupled transient climate-ice sheet simulations

To test the response of the Northern Hemisphere ice sheets to different ablation parameterisations, we first carried out a set of three transient simulations from 126 to 0 ka with the three PDD models described in Sect. 2.4 (see Table 1). These experiments have been run with the fully coupled CLIMBER-GRISLI model in order to account for the main interactions between ice sheets and other components of the climate system operating over millennia. The model is initialised with a 5000 yr equilibrium run performed under 126 ka conditions of insolation and CO_2 . We assumed that the initial ice-sheet configuration was identical to the present-day Greenland geometry. During transient simulations, the model is forced by

variations of insolation (Laskar et al., 2004), CO₂ (Petit et al., 1999) and sea level (Waelbroeck et al., 2002). In this model configuration, the ice-sheet model is called every 20 yr and is run during 20 yr.

Figure 1 displays the spatial distribution of the Northern Hemisphere ice sheets at 116 and 21 ka simulated with the three PDD models. The most striking result is the small amount of ice built by the RH91 (run 1) and TP02 (run 2) models, especially at the last glacial maximum (LGM) where the only ice-covered regions are the Ellesmere Island and parts of the Canadian Archipelago and of the Rocky Mountains. Moreover, none of these models succeeds in simulating ice over Fennoscandia. These results are particularly surprising when compared to the reconstructed extents of the LGM ice sheets (e.g., Peltier, 2004). By contrast, reasonable glacial inception is obtained with the FST09 model (run 3). At 116 ka, the ice-equivalent sea-level drop coming from the only contribution of Northern Hemisphere ice sheets is ~ 18 m in agreement with sea-level reconstructions (Bintanja et al., 2002; Waelbroeck et al., 2002). At the LGM the simulated ice volume of boreal ice sheets reaches $47.8 \times 10^{15} \text{ m}^3$, a value close to $49.7 \times 10^{15} \text{ m}^3$ provided by the ICE-5G reconstruction (Peltier, 2004). The mean areal coverage of LGM ice sheets is also favourably compared with available reconstructions (Peltier, 2004; Lambeck et al., 2006; Tarasov et al., 2012) except for the insufficient Southeastern extent of the North American ice sheet and the absence of the Barents-Kara ice sheet. These results clearly show that in the CLIMBER-GRISLI model, the FST09 PDD parameterisation favours glacial inception over the Northern Hemisphere.

Owing to the spatial resolution of CLIMBER, these results are quite satisfactory. However, the simulated glacial-interglacial cycle presents some unrealistic features. As an example, although the first glaciation step over Scandinavia occurs as early as 120 ka, the actual glacial inception of the Fennoscandian ice sheet does not take place before 30 ka, in contradiction with many paleo-indicators and geomorphological reconstructions (see Svendsen et al., 2004 for a detailed review). Moreover, in these standard simulations, there is no complete deglaciation at 0 kyr BP. Previous studies suggest that an increase of climatic variability (Bonelli et al., 2009) or the impact of dust deposition on snow albedo (Ganopolski et al., 2010; Bonelli et al., 2009) may have played a critical role in the deglaciation process. Here, for simplicity reasons and to compare more easily the impact of different ablation parameterisations, we have chosen to keep σ constant through time and not to include a representation of the impact of dust on snow albedo. Moreover, in the present version of GRISLI, the impact of water-saturated sediments on basal sliding that favours the ice retreat has not been taken into account. These missing mechanisms may explain why the last glacial termination is not simulated satisfactorily in our experiments. Our following analysis therefore focuses on the 126–21 ka period. Our aim here is not yet to simulate a perfect picture of the last glacial-interglacial cycle in full

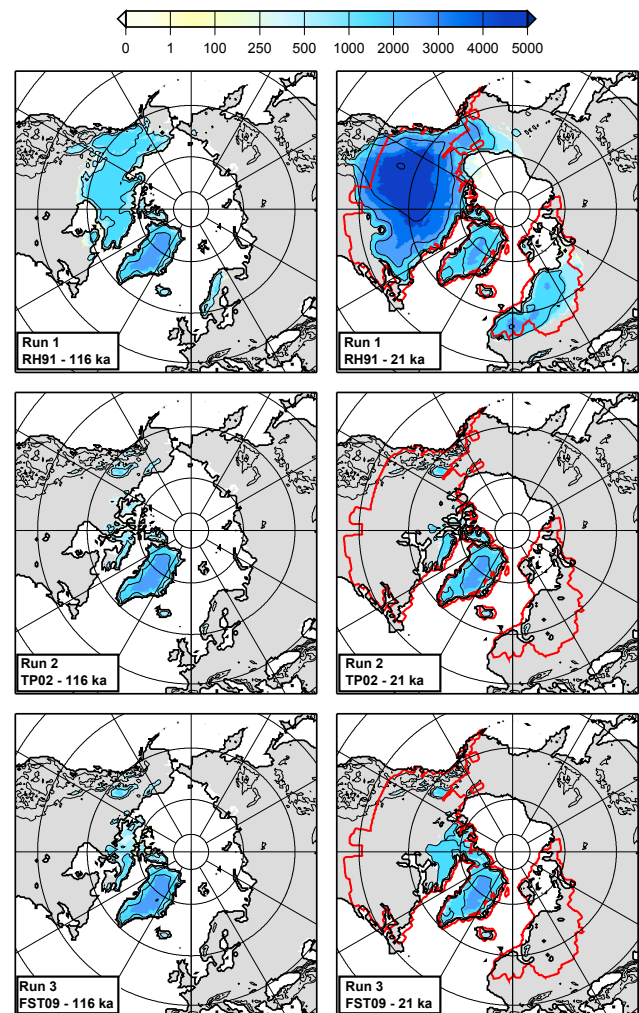


Fig. 1. Simulated ice thickness (in m) at 116 ka (left panels) and 21 ka (right panels) produced by the three standard fully coupled experiments with the RH91 (run 1, top panels), TP02 (run 2, middle) and FST09 (run 3, bottom) PDD models. Thick black lines represent the coastline and thin black lines display the iso-contours of surface elevation (from 1000 to 5000 m). The thick red lines in the right panels represent the areal extent of the ICE-5G LGM ice sheets (Peltier, 2004).

agreement with all available paleodata, but rather to examine the extent to which the evolution of Northern Hemisphere ice sheets throughout this time period is linked to the ablation parameterisation (and, therefore, to the choice of the PDD model) or to the climate-ice sheet feedbacks. These issues are addressed in the following sections through GRISLI equilibrium experiments and CLIMBER-GRISLI sensitivity studies.

Table 2a. GRISLI equilibrium simulations: present-day.

Climate Forcings	Initial topography conditions	PDD Models	Run ID
Present-day (from CLIMBER experiment with CO ₂ = 360 ppm)	Present-day	RH91, TP02, FST09	4, 5, 6
Present-day (from ERA-Interim)	Bamber et al. (2001)	RH91, TP02, FST09	7, 8, 9

Table 2b. GRISLI equilibrium simulations: past periods

Climate Forcings (from time-slice CLIMBER experiments)	Initial topography conditions (from std FST09 experiments)	PDD Models	Run ID
120 ka	120 ka FST09	RH91, TP02, FST09	10, 11, 12
112 ka	112 ka FST09	RH91, TP02, FST09	13, 14, 15
21 ka	21 ka FST09	RH91, TP02, FST09	16, 17, 18

4.2 GRISLI equilibrium simulations

4.2.1 Present-day simulations

In the previous section, we have shown that the FST09 PDD formulation provides a more realistic geometry of LGM ice sheets with respect to available reconstructions (Peltier, 2004; Lambeck et al., 2006; Tarasov et al., 2012). However, these results are likely to be model-dependent. To investigate the impact of potential CLIMBER biases on the current results we carried out GRISLI simulations (see Table 2a) forced during 50 kyr with the present-day climate given either by CLIMBER (runs 4 to 6) or by the ERA-interim database (Dee et al., 2011) (runs 7 to 9). These runs have been performed with the three PDD models without accounting for ice-related feedbacks. The initial ice-sheet topography is given by Bamber et al. (2001): data of ice thickness and bedrock elevation are interpolated on a 5 km × 5 km grid. This gives to an estimation of the Greenland ice volume $2.93 \times 10^{15} \text{ m}^3$. When interpolated on the GRISLI grid, the same dataset leads to a reduced ice volume of $2.88 \times 10^{15} \text{ m}^3$, denoted V_{ref} in the following. This latter ice volume lies within the range of $2.83\text{--}2.97 \times 10^{15} \text{ m}^3$ given by various sensitivity experiments to model parameters in Ritz et al. (1997).

Figure 2 represents the magnitude of the ice volumes and the ice-covered areas obtained at the end of the simulation, when the equilibrium is reached. This figure shows that the simulated ice volume is larger when GRISLI is forced by climatic variables coming from ERA-Interim. This is directly related to larger accumulation rates (w.r.t. the CLIMBER climate forcing) over the entire Greenland ice sheet, especially

over the southeastern margin (not shown). By contrast, simulated ice-covered areas are larger when the climate computed by CLIMBER is used as input to GRISLI due to colder summer air temperatures (w.r.t. ERA-Interim) that reduce ablation at the ice sheet margins (not shown). This figure also illustrates that in both cases (i.e., CLIMBER and ERA-Interim climate forcings), the FST09 model provides a larger ice volume than the other PDD models. When forced by the reanalysis (run 9), the FST09 ice volume is 9 % greater than the V_{ref} ice volume derived from observations (Bamber et al., 2001), while the RH91 and TP02 models (runs 7 and 8) simulate ice volumes in a very good agreement with V_{ref} with less than 1 and 2 % differences. However, when forced by CLIMBER, these two latter models (runs 4 and 5) underestimate the present-day V_{ref} value by as much as 8 and 6 % respectively, while the FST09 ice volume (run 6) only differs from V_{ref} by less than 1 %. Therefore, under present-day climatic conditions, the FST09 PDD model allows to compensate for the climatic biases of CLIMBER over Greenland.

4.2.2 Simulations of past periods

Additional GRISLI equilibrium simulations have been carried out to investigate the sensitivity of the simulated ice sheets to the choice of the PDD parameterisation during past periods. Similarly to experiments 4 to 6 presented in the previous section, GRISLI has been forced during 50 kyr by the CLIMBER climatic outputs (see Table 2b) coming from 10 kyr time-slice experiments (i.e., under conditions of insolation and CO₂ constant through time). The change of temperature and snow accumulation with the altitude is not taken into account. These simulations have been carried out for

Table 3. Sensitivity experiments to PDD parameters.

Forcings	Insolation CO ₂ Sea level	Laskar et al. (2004) Petit et al. (1999) Waelbroeck et al. (2002)		
Initial Conditions	126 kyr climate Present-day Greenland topography			
Standard deviation σ	DDF Cice, Csnow	Refreezing Scheme	Run ID	
FST09	RH91	TP02	19	
FST09	TP02	RH91	20	
Fixed: 5 °C	FST09	FST09	21	
FST09	Fixed: RH91 values	FST09	22	
RH91		FST09	23	
FST09	FST09	TP02	24	
FST09	FST09	RH91	25	

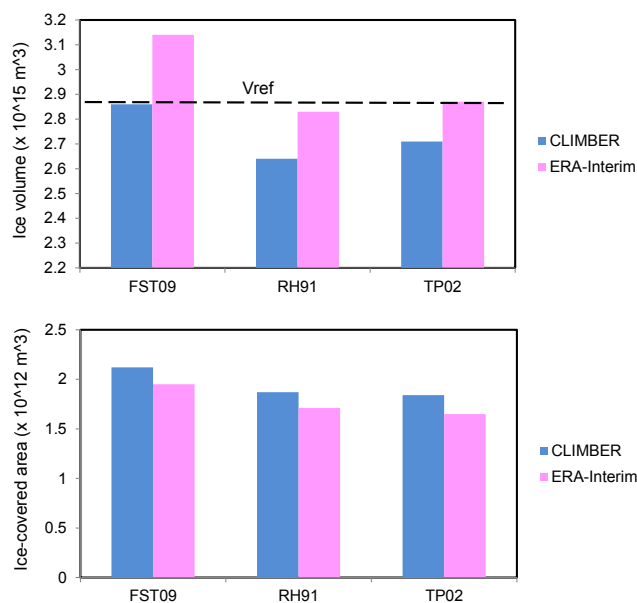


Fig. 2. Magnitude of the ice volumes (top panel) and ice-covered areas (bottom panel) obtained at the end of the present-day simulations forced either with CLIMBER (runs 4 to 6) or with the climatic variables coming from the ERA-Interim dataset (runs 7 to 9). The dotted black line in the top panel represents the magnitude of the initial ice volume ($V_{\text{ref}} = 2.88 \times 10^{15} \text{ m}^3$) coming from Bamber et al. (2001) and interpolated on the GRISLI model grid.

different key periods of the last glacial-interglacial cycle (i.e., 120 ka, 112 ka and 21 ka) in order to investigate the model sensitivity to different PDD formulations in various combinations of insolation and ice volume. The 120 ka period corresponds roughly to the onset of glaciation, while the 65° N summer insolation is still at a relatively high level. The second period (i.e., 112 ka) corresponds to a low insolation level.

At that time, reconstructions based on benthic $\delta^{18}\text{O}$ suggest that sea level had dropped by $\sim 40\text{--}50$ m (Waelbroeck et al., 2002) and, thus, that ice volume was at an intermediate level compared to the LGM where sea-level was lowered by ~ 120 m. At 21 ka, ice volume was at or close to its maximum, while insolation was close to present-day setting. The ice-sheet boundary condition of the CLIMBER runs, used also as an initial condition of the 50 kyr GRISLI experiments, are taken from the fully coupled standard FST09 experiment (i.e., run 3). This choice is motivated by the ability of the FST09 PDD model to produce a reasonable ice volume evolution through the last glacial period. Each PDD parameterisation described in Sect. 2.4 has been used to compute the surface mass balance of the ice sheets.

Figure 3 displays the evolution of the simulated ice volumes and ice-covered areas inferred from the three PDD formulations for 120 (runs 10 to 12), 112 (runs 13 to 15) and 21 ka (runs 16 to 18). A common feature observed in these plots for the three periods is that the FST09 model clearly amplifies the glaciation process. Moreover, the ice-covered area simulated with RH91 and TP02 rapidly decreases during the first time step of the simulation. This means that these latter PDD models are unable to maintain the FST09 ice-sheet given by run 3 as initial state. The largest differences in both ice volumes and ice covered areas are observed for 120 ka (Fig. 3) with a glaciation process clearly amplified with the FST09 model (run 12). At the end of the simulation, the ice-covered areas and the ice volumes simulated with FST09 are respectively 25 % (26 %) and 43 % (32 %) larger than those simulated with RH91 (TP02) in runs 10 and 11. To understand the response of the simulated ice sheets, it is necessary to carefully examine the different PDD components for the same ice-sheet reference (i.e., ice-covered area and altitude). Therefore, for each period, we computed off-line the amount

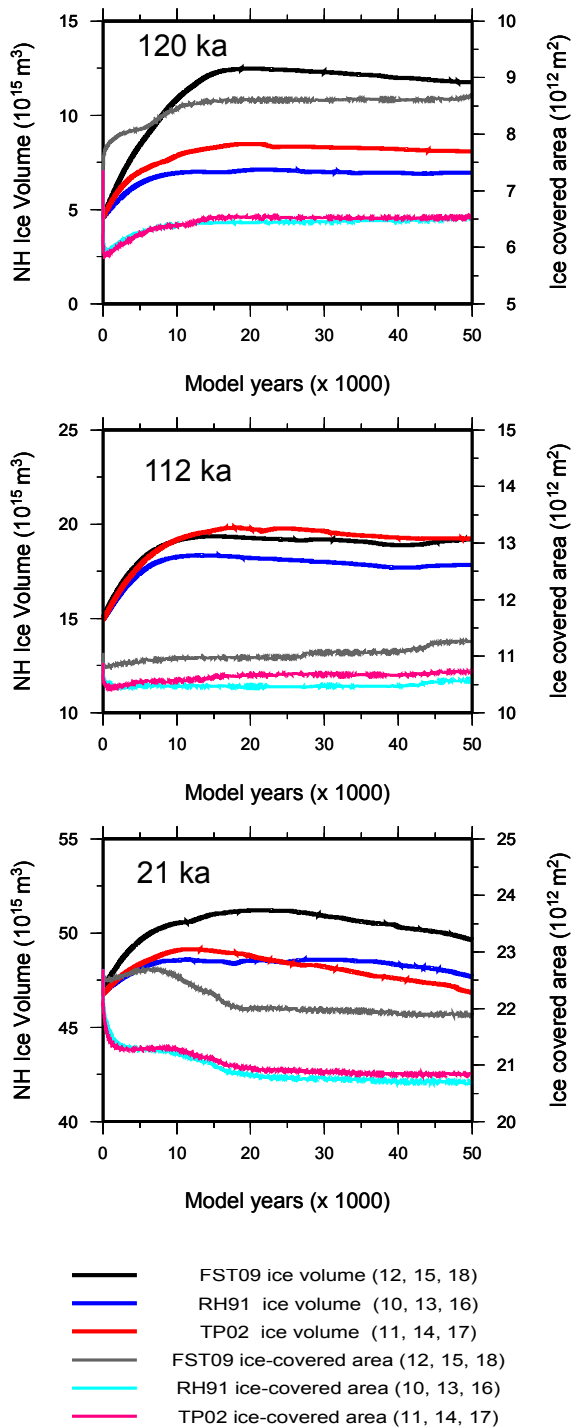


Fig. 3. Evolution of the simulated ice volumes (thick solid lines) and ice-covered areas (thin solid lines) in the GRISLI equilibrium experiments run with the three PDD models. In these experiments, GRISLI is forced by CLIMBER snapshots for 120, 112 and 21 ka (see Table 2b and text for a comprehensive description of the experiments). Numbers in parenthesis refer to the run identifiers (runs 10 to 18).

of ablation and ice refrozen mass for a reference ice sheet (Fig. 4) given by the FST09 ice sheet (run 3).

Figure 4 shows that for a given ice surface the ablation computed with the FST09 model is smaller than the ablation computed with any of the two other PDD models. This feature is particularly pronounced at 120 ka (20 and 13 % the RH91 and TP02 ablation) and to a lesser extent at the LGM (39 and 30 %, respectively). Owing to the small amount of refreezing, this small ablation rate is not related to the contribution of superimposed ice. Therefore, the origin of the large FST09 ice volume is linked to the greater ice expansion, which is itself due to the parameterisation of the standard deviation of temperature distribution, accounting for daily and inter-annual temperature variability. As an example, when the altitude of the ice sheet is around 500 m, the σ value is 2.2°C , whereas it is 5 and 5.2°C in RH91 and TP02 models, respectively. In fact the larger the variability, the larger the probability of having positive temperatures in a given day is, favouring thereby the ablation process. Therefore, these results suggest that during glacial inception, the surface mass balance of ice sheets is critically dependent on temperature variability.

The comparison of the results obtained with RH91 (run 10) and TP02 (run 11) shows that the ice-covered area simulated with RH91 is almost equivalent to that simulated with TP02 for the three periods under study. However, the values of ablation and refreezing present some large differences from one model to the other (Fig. 4). At 120 ka, the amounts of ablation and refreezing computed with TP02 are respectively 1.5 and 3.3 larger than those computed with RH91. In the same way, at 112 ka, the TP02 and FST09 ice volumes follow similar evolutions with ablation/refreezing values computed for the ice-sheet reference ranging from $3.0/0.8 \times 10^{11} \text{ m}^3 \text{ yr}^{-1}$ (FST09) to $12.8/49.2 \times 10^{11} \text{ m}^3 \text{ yr}^{-1}$ (TP02). The TP02 experiment has an excess of refreezing relative to ablation. The opposite situation is observed in the FST09 run, but the excess of ablation is offset by enhanced accumulation from expanded ice-covered area (Fig. 3). A similar situation is finally observed at 21 ka with RH91 (run 15) and TP02 (run 16) ice volumes of similar magnitude while ablation/refreezing values are rather different. These results illustrate that the different PDD formulations used for climates different from the present-day one may produce similar ice volumes or ice-covered areas with rather different combinations of ablation and refreezing components (Fig. 4).

A second striking result lies in the huge amount of TP02 refreezing compared to those computed with RH91 and FST09: the amount of refrozen ice may be 3 to 15 times greater than that computed with RH91 and between 63 to 68 times greater the FST09 one depending on the period. This is apparently in contradiction with the results of Reijmer et al. (2012) who found that the Janssens and Huybrechts model (2000), similar to TP02, predicts less refreezing than the RH91 model. This contradiction may be partly explained by small differences in the thickness of the thermally active

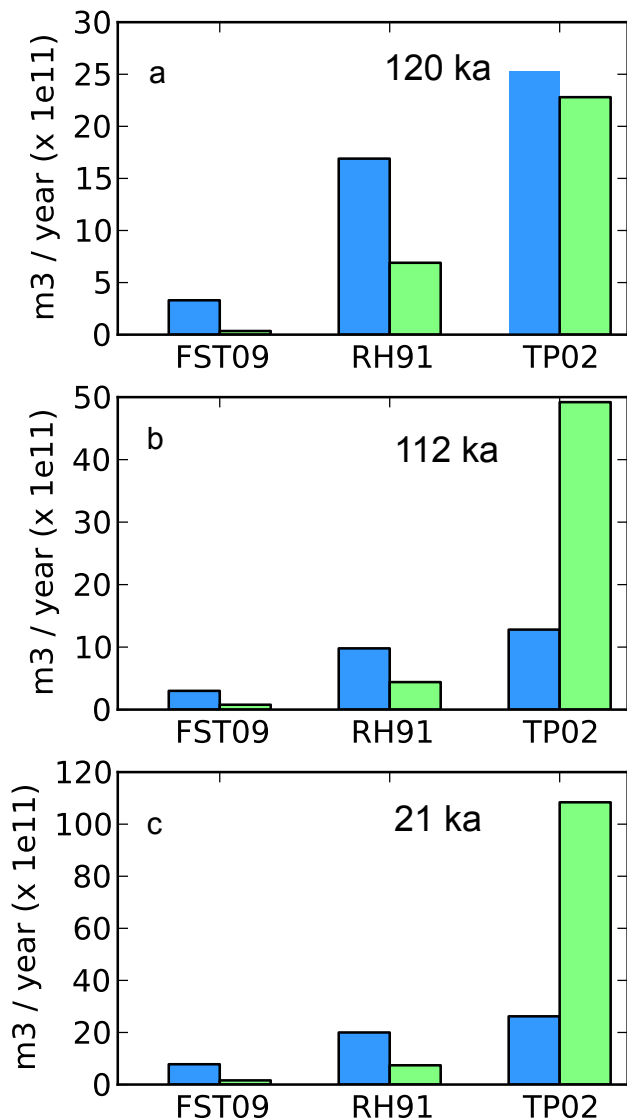


Fig. 4. Amounts of ablation (blue) and refrozen ice (green) given in $\text{m}^3 \text{yr}^{-1}$ computed with the three PDD models for 120 (a), 112 (b) and 21 ka (c). These amounts are calculated for the same ice-sheet surface given by the FST09 standard simulation (run 3).

layer (see Sect. 2.4) and by the fact that the analysis of Reijmer et al. (2012) is focused on the 1958–2008 period. In our study, the large excess of TP02 refreezing is slightly reduced under present-day conditions, but still remains 2.6 times larger than the RH91 refreezing.

Another important key point relies on the similarity between spatial distributions of ice sheets simulated with the three PDD models at 112 and 21 ka (not shown). This suggests that their response is strongly influenced by the initial topography condition given by the fully coupled FST09 simulation (run 3). By contrast, at the onset of glaciation (i.e., at 120 ka), the initial amount of ice is too small to exert a noticeable control on the simulated ice sheets. Therefore, dur-

ing this time period, the response of the ice sheets seems to be mainly governed by the ablation method and more specifically by the amplitude of temperature variations, as previously illustrated.

Our results demonstrate the complexity of the ice sheet response to a given climatic forcing. It also illustrates the need to identify how each PDD component comes into play and the relative influence of ablation and feedback processes. These issues are addressed in the following sections through several sets of sensitivity experiments.

5 Sensitivity studies

5.1 Role of PDD parameters

The third series of simulations is designed to investigate the relative influence of PDD parameters on simulated ice sheets over the last glacial-interglacial cycle. These experiments have been carried out following the same experimental setup as the first series except for the PDD parameters that have been exchanged one by one from one PDD formulation to the other. As an example, the FST09 model has been run with DDF parameters, retention scheme and standard deviation coming from RH91. A similar procedure has been followed with the two other formulations with the appropriate exchange of parameters (see Table 3 for a summary of these simulations).

The fundamental question arising from results discussed in previous sections is why the FST09 model leads to a reasonable evolution of the ice volume through the last glacial cycle compared to the RH91 and TP02 models. The analysis of the GRISLI equilibrium simulations has shown that the simulated ice-covered area is enhanced with the FST09 PDD formulation. This suggests that the parameter representing the variability of temperatures plays a significant role in the glacial inception process especially at low altitudes, which, in turn, favours the further development of Northern Hemisphere ice sheets through ice-related feedbacks (see Sect. 5.2). To confirm this assumption, we have replaced the σ altitude relationship used in FST09 with the fixed value of the σ parameter used in RH91 and TP02 (run 21). The net consequence is that the model is no longer able to produce ice over Northern Hemisphere areas (Fig. 5) with the exception of tiny portions in the Rocky Mountains and near Baffin Bay. This clearly demonstrates the huge impact of the representation of stochastic variations of temperature on the construction of Northern Hemisphere ice sheets. Besides, when the σ altitude relationship is used in RH91 and TP02 models (runs 19 and 20), the entire GRISLI domain becomes ice-covered (Fig. 5). This yields to an LGM ice volume 28 (resp. 22) times larger than the RH91 (resp. TP02) one obtained in the standard experiment and 1.4 (resp. 1.6) times larger than the FST09 one at the LGM. Neglecting the dependency of σ on the altitude in these models, as in the standard

simulations (runs 1 and 2), could be therefore at the origin of the small amount of ice simulated over locations of past ice sheets. However, the results obtained with these new formulations are now completely unrealistic. Such results can be explained by the large amount of refreezing produced by TP02, and to a lesser extent by RH91. When combined with the σ altitude relationship, these large amounts of refreezing cause a massive glaciation as well.

These overall results also suggest that in the FST09 model, the effect of the dependency of the σ parameter on altitude is counterbalanced either by the refreezing scheme or by DDF factors. Substituting the DDF-temperature relationship used in FST09 by fixed values (as in RH91) does not lead to significant changes (less than $\sim 3\%$) in simulated surface mass balances (run 22), although the standard FST09 model tends to slightly enhance the ablation (not shown). Same kind of conclusions can be drawn from the use of DDF-temperature dependency (as prescribed in FST09) in the RH91 model (run 23). Therefore, as suggested in previous sections, the method for computing the amount of superimposed ice seems to be a good candidate to counteract the effect of the temperature variability.

To confirm this assumption, two additional experiments have been carried out by changing the refreezing scheme in the FST09 model. The use of the TP02 refreezing formulation in FST09 (run 24) leads to a strong increase of the ice thickness of more than 1000 m over the North American and Scandinavian ice sheets at 115 ka, and to a southward expansion of the ice (Fig. 6a). At 21 ka, the ice thickness increases over the major part of both Greenland and Canada, except in the western part. More surprising is the growth of ice all over the eastern part of the GRISLI domain (Fig. 6b). This pattern is fully correlated with the spatial distribution of the ice sheets simulated with the TP02 model when the fixed standard deviation of temperature distribution is replaced with the σ altitude relationship as used in FST09 (run 20, Fig. 5), and corresponds to a 94 % ice volume increase with respect to the standard FST09 case (run 3). Using a Pmax value fixed to 0.6 (as in RH91) in the FST09 model (run 25) leads to similar results (with an amplification of the ice volume of 40 %) except over Greenland where ice thickness decreases (Fig. 6c–d). This is likely due to the cooling effect induced by the growth of the adjacent Canadian ice sheet which causes a depletion of snow accumulation probably amplified by the coarse spatial resolution of CLIMBER. The depletion of snow accumulation cannot be produced by a displacement of planetary waves in response to orographic and/or thermal effects since their parameterisation has been removed from the present model configuration. Moreover, the decrease of snow accumulation is not totally counteracted by the amount of refreezing which remains smaller than the TP02 one.

These sensitivity experiments help to identify the relative importance of each PDD parameter in the evolution of past Northern Hemisphere ice sheets. The effect of temperature

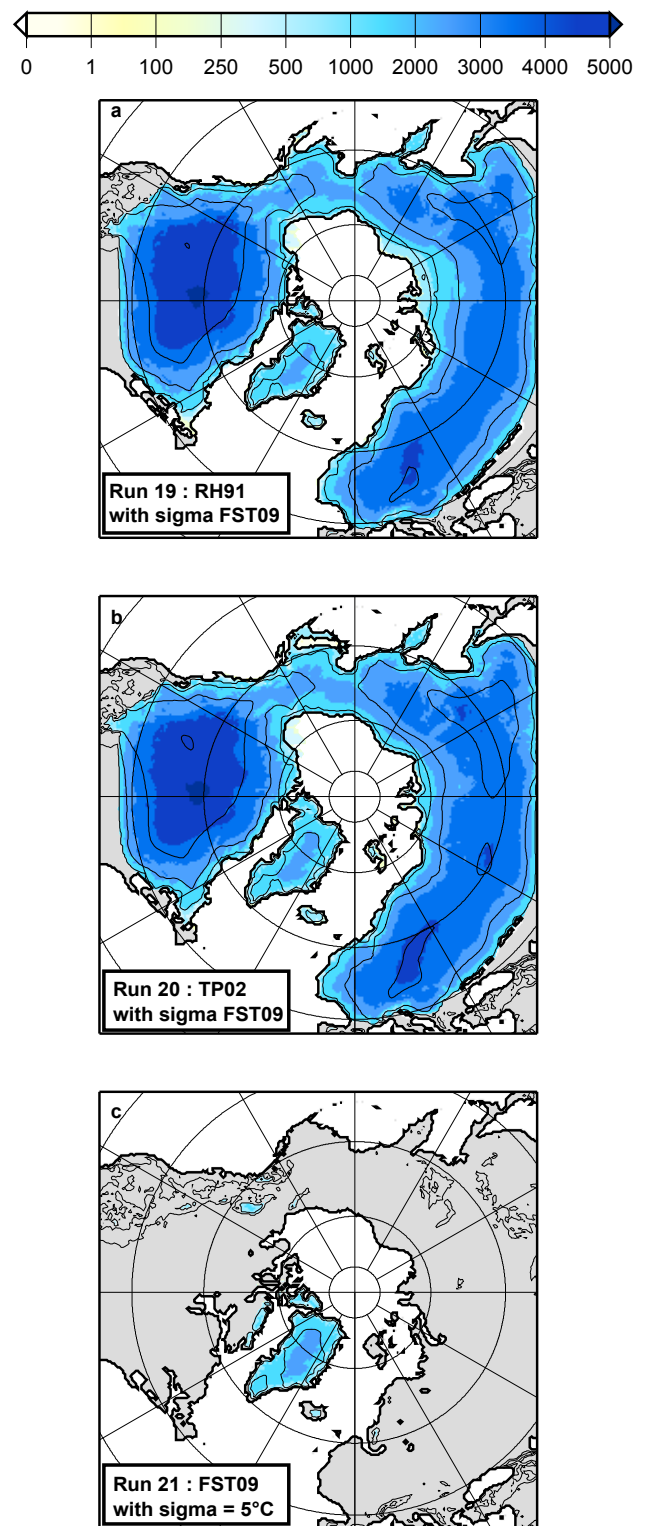


Fig. 5. Simulated ice thickness at 21 ka (in m) obtained by substituting the FST09 σ altitude relationship in RH91 (a, run 19) and TP02 (b, run 20) models, and when using a fixed ($= 5.0^\circ\text{C}$) σ value in the FST09 model (c, run 21).

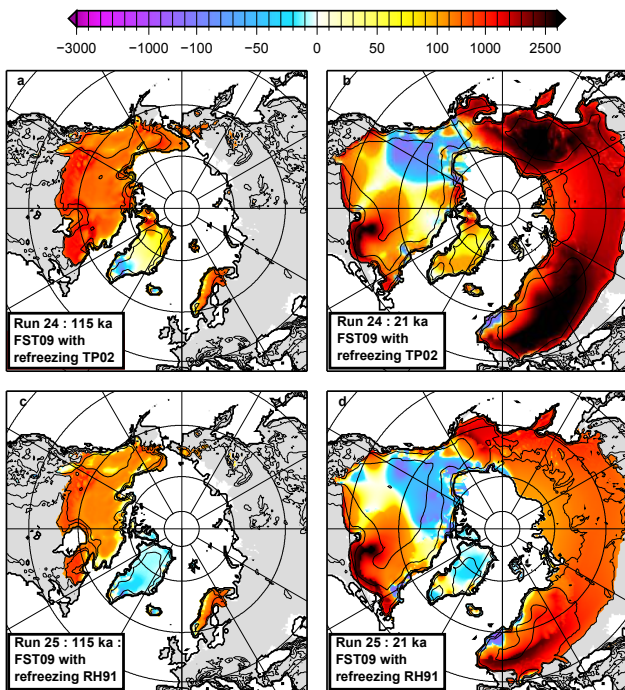


Fig. 6. Simulated ice thickness difference (in m) when substituting the TP02 refreezing scheme in the FST09 model (FST09–FST09 with TP02 refreezing, top panels, run 24), and when allowing in the FST09 model a fixed portion (i.e., $P_{\max} = 60\%$) of meltwater to produce superimposed ice (FST09–FST09 with RH91 refreezing, bottom panel, run 25). Left panels refer to the 115 ka period and right panels refer to the LGM (i.e., 21 ka). The thick black lines represent the contour of the continents and the thin ones display the iso-contours of surface elevation (from 1000 to 5000 m).

variability appears to be dominant though modulated by the amount of refreezing. The other main processes that likely play a significant role in the development of the ice sheets are linked to ice-related feedbacks (i.e., albedo and/or altitude effect). In the following section, we examine how a change in ice-sheet configuration at different key periods of the last glacial cycle may influence the further evolution of Northern Hemisphere ice sheets.

5.2 Role of the ice-sheet geometry

Since the FST09 model favours ice expansion in the early phase of glacial inception, ice-sheet feedbacks may amplify the glaciation process. As a consequence the direct comparison of the different PDD models may lead to a misinterpretation of their ability to produce a reasonable evolution of Northern Hemisphere ice sheets through the last glacial cycle. To investigate how the construction of simulated Northern Hemisphere ice sheets throughout the last glacial cycle may be impacted by the shape and size of ice sheets themselves at given stages of the simulation, an additional series of experiments has been carried out with different initial

conditions of ice-sheet topography and different PDD models (Table 4). These experiments start respectively at 115 ka close to the insolation minimum (runs 26 to 28), 60 ka, corresponding to a full glacial state period (runs 29 to 31) and 30 ka which marks a new glaciation phase (runs 32 to 34). All these experiments are run with both RH91 and TP02 models with an initial climatic state and an initial ice-sheet topography given by the fully coupled FST09 simulation at these key periods.

The evolution of the simulated ice volumes (Fig. 7) clearly shows that the presence of a larger ice sheet at 115 ka (runs 26 and 27) enables the ice volume to increase and to reach greater values ($\sim 22 \times 10^{15} \text{ m}^3$ at the LGM) than those obtained in the TP02 and RH91 standard simulations ($\sim 2\text{--}3 \times 10^{15} \text{ m}^3$). This means that at some key periods of the last glacial cycle, such as the onset of glaciation, a rather large ice sheet seems to be a crucial element to ensure a reasonable further build-up of the North American ice sheet. This also underlines the potential impact of ice-sheet feedbacks. However, ice volumes simulated with RH91–115FS (run 26) and TP02–115FS (run 27) experiments are about 45 % smaller than the one provided by the standard FST09 simulation (run 3). This demonstrates that, at the onset of glaciation, a change in ice-sheet configuration may approximately explain half of the LGM ice volume.

Experiments starting at 60 ka (resp. 30 ka) with the FST09 initial conditions and run with the RH91 and TP02 models (runs 28–29 and 32–34) do not show a substantial increase of the ice volume after 60 ka (resp. 30 ka). This suggests that the amplitude of the feedback of the initial FST09 ice sheet on the climate is not large enough to produce an evolution of the ice volume similar to that obtained in the standard FST09 simulation (run 3). Moreover, after the LGM, located at around 17 ka in our simulations, the ice volume tends to decrease. Compared to results provided by the standard FST09 experiment, this confirms that, in our model configuration, the RH91 and TP02 PDD formulations favour the ablation and suggests that the influence of initial ice-sheet conditions is of secondary importance.

To better assess the impact of the initial ice-sheet geometry, we performed additional tests in which the transient simulation of the last glacial cycle was initialised with standard TP02 ice sheets (i.e., simulated in run 2) at 115, 60 and 30 ka. Surprisingly, although the 115 ka starting point is characterised by a small initial amount of ice, the further evolution of the ice volume is similar to that of the standard FST09 experiment (run 3). Similarly, a significant ice growth is observed in the experiments starting with the 60 and 30 ka TP02 ice sheets and run with the FST09 model (runs 31 and 32). These results confirm the ability of the FST09 model to produce glacial inception at any stage of the last glacial cycle through rapid expansion of ice in response to insolation and CO_2 forcings.

These sensitivity experiments show that the relative impact of both ablation related processes and ice-sheet feedbacks in

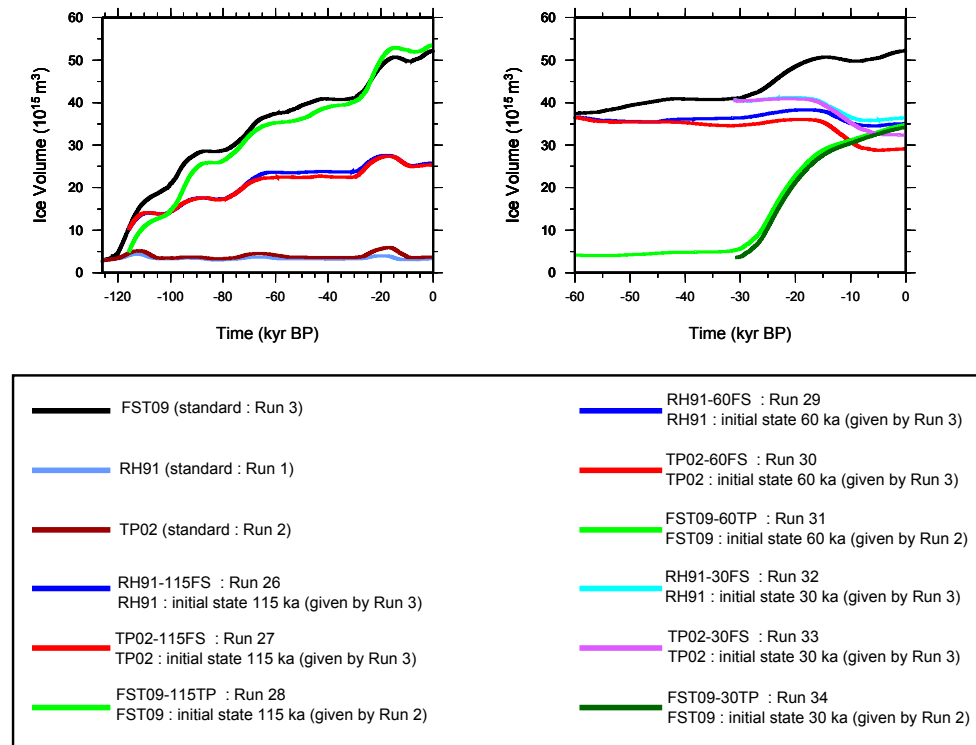


Fig. 7. Simulated ice volumes in runs 26 to 34 (and compared to the ice volumes obtained in the standard experiments: runs 1 to 3) to test the impact of the ice-sheet feedbacks. Different initial conditions are considered at 115 ka (left panels) and 60 and 30 ka (right panels) with initial ice-sheets given either by the standard FST09 simulation (experiments referring to as Xi-YiFS) or by the standard TP02 simulation (Xi-YiTP).

the evolution of Northern Hemisphere ice sheets throughout the last glacial cycle is strongly dependent on the PDD formulation. In experiments run with PDD models that favour ablation, the large initial ice sheet given by the standard FST09 simulation is responsible for about half of the LGM ice volume. On the other hand, when ablation is limited due to low temperature variability, these feedbacks do not appear so crucial. In such a situation, the evolution of the ice system is dominated by the impact of daily or inter-annual amplitude of temperature variations.

6 Conclusions

Since the development of coupled climate-ice sheet models, the reliability of the PDD method to compute ablation has been more and more questioned in the literature. This method accounts for the melt-temperature relationship, but ignores the effect of insolation variations and albedo on snow and ice materials. This implies the non-universality of the PDD method both in space and time. With this respect, van de Berg et al. (2011) recently underlined that the use of the PDD approach was not appropriate in a paleo-climatic context. Energy balance models appear more physically-based, but suffer from a lack of constraints, despite first attempts made for

simulations of past periods (Ganopolski et al., 2010; Robinson et al., 2011; Fyke et al., 2011). Regional atmospheric models coupled with physical snow models (e.g., Lefebvre et al., 2005; Ettema et al., 2009; Fettweis, 2011, 2013; Reijmer et al., 2012) offer a detailed representation of atmospheric and metamorphic processes of snow and ice. Such models have been validated against observations of present-day Greenland. Unfortunately, due to their high computational cost, they cannot be used at the 100 kyr time scale. Therefore, the empirical PDD formulation is still the most common approach to study the climate-ice sheet system over multi-millennia time periods. Within this context, the uncertainties linked to this approach appear as a key issue.

In the present study, we used the coupled CLIMBER-GRISLI model to evaluate the sensitivity of the simulated geometry of ice sheets to the PDD formulation. Our different series of experiments shows that our model is highly sensitive to the PDD model with very different responses observed from one formulation to the other. In particular, it has been shown that at some key periods, change in any PDD parameter may notably modify the overall glacial cycle. The relation between DDF coefficients C_{ice} and C_{snow} with temperature seems to only have a small impact, at least for the period under study. Conversely, the surface mass balance of Northern Hemisphere ice sheets appears to be strongly dependent

Table 4. Sensitivity experiments to ice-sheet topography.

Forcings	Insolation CO ₂ Sea level	Laskar et al. (2004) Petit et al. (1999) Waelbroeck et al. (2002)	
Initial Conditions	126 kyr climate Present-day Greenland topography		
Climatic and topography initial conditions	PDD Models	Run duration (× 1000 yr)	Run ID
Given by Run ID 3 at 115 ka (standard FST09)	RH91	115	26 (RH91-115FS)
Given by Run ID 3 at 115 ka (standard FST09)	TP02	115	27 (TP02-115FS)
Given by Run ID 2 at 115 ka (standard TP02)	FST09	115	28 (FST09-115TP)
Given by Run ID 3 at 60 ka (standard FST09)	RH91	60	29 (RH91-60FS)
Given by Run ID 3 at 60 ka (standard FST09)	TP02	60	30 (TP02-60FS)
Given by Run ID 2 at 115 ka (standard TP02)	FST09	60	31 (FST09-60FS)
Given by Run ID 3 at 60 ka (standard FST09)	RH91	30	32 (RH91-30FS)
Given by Run ID 3 at 60 ka (standard FST09)	TP02	30	33 (TP02-30FS)
Given by Run ID 2 at 60 ka (standard TP02)	FST09	30	34 (FST09-30FS)

on the representation of temperature variability, mainly at the onset of glaciation. In turn, this may have a crucial impact for subsequent build-up of ice sheets, depending on the way this variability is accounted for in the PDD model. The parameterisation of the standard deviation σ as a function of the elevation, recommended by Fausto et al. (2009), decreases the ablation at the edges of ice sheets and favours the glaciation of low altitude areas. This response is nevertheless modulated by the refreezing process. In our model, the use of the FST09 parameterisation of σ in combination with a refreezing scheme leading to a large amount of superimposed ice yields a massive glaciation with a 1.4 to 1.6 increase of the LGM ice volume, in total disagreement with sea-level and geological reconstructions (Bintanja et al., 2002; Brigham-Grette, 2001; Lambeck and Chapell, 2001; Lambeck et al., 2006; Peltier, 2004; Tarasov et al., 2012; Svendsen et al., 2004; Waelbroeck et al., 2002). Conversely, a large amount of superimposed ice is not a sufficient condition to properly simulate the ice sheet evolution throughout the last glacial cycle and may lead to a 40 to 94 % ice volume increase at the LGM compared to that obtained in the standard FST09 experiment. Therefore, our study shows that the use of the PDD approach in climatic conditions fully different from the present-day ones requires an appropriate calibration of the

PDD parameters. This calibration is likely to be strongly dependent on the climate-ice sheet model. However, we emphasise again that this study has not been designed to define the best PDD model. Its aim is rather to underline the respective roles of each PDD parameter in a paleo-climatic context and to determine the relative impact of processes relying on the representation of ablation and ice-sheet feedbacks. Here, it clearly appears that the FST09 formulation provides a more realistic geometry of LGM ice sheets with respect to available reconstructions (e.g., Peltier, 2004). However, these latter results are likely to be model-dependent. In fact, a cooler climate model could produce a reasonable glaciation with the RH91 and TP02 approaches, as suggested by the GRISLI equilibrium simulations forced with the ERA-Interim climatic variables (Dee et al., 2011), and a too massive glaciation with FST09.

None of the PDD formulation used in this study enables us to simulate the last glacial termination. This major drawback may come from missing mechanisms and/or the improper representation of some processes, such as those relying on basal sliding and fast ice flow. However, this study highlights the importance of the σ parameter and clearly suggests that the role of stochastic variations of temperature should be carefully considered in any further study. The

parameterisation suggested by Fausto et al. (2009) has been inferred from observations made for the present-day Greenland ice sheet. Nonetheless, the universality of this relationship is unlikely. Therefore, a calibration of the σ parameter as a function of space and time could be considered as a mean to improve the simulation of the last deglaciation, in line with previous findings made by Bonelli et al. (2009).

It should finally be emphasised that detailed snow models coupled to regional atmospheric models could provide a reasonable set of PDD parameters. A pioneering study conducted by Reijmer et al. (2012) examined different re-freezing schemes forced by climatic fields simulated by the RACMO2 and MAR models. The results were compared to outputs from these both models in which the refreezing process is explicitly computed. Such approaches should also be applied to the temperature variability (i.e., standard deviation of the PDD distribution) from the daily to the inter-annual time scale. The variations of melt rate factors (i.e., DDF) could be more thoroughly studied by running advanced energy balance models including a detailed snow scheme, for which outputs could be directly compared to observations, as proposed earlier by Braithwaite (1995). The development of similar studies conducted with different models could help to better constrain the temporal and geographical variations of the PDD parameters and, thus, to provide a better calibration of the PDD formulations, which are still commonly used in the climate-ice sheet modelling community.

Acknowledgements. The authors are very grateful to Roger Braithwaite and Lev Tarasov for their constructive comments that allowed to improve the writing of the manuscript. Chris Stokes is also thanked for his editorial advices. This work has benefited from the useful contribution of Jean-Yves Peterschmitt and Pauline Beghin in doing the figures. This study was supported by CEA, CNRS and UVSQ.

Edited by: C. R. Stokes



The publication of this article is financed by CNRS-INSU.

References

- Abe-Ouchi, A., Segawa, T., and Saito, F.: Climatic Conditions for modelling the Northern Hemisphere ice sheets throughout the ice age cycle, *Clim. Past*, 3, 423–438, doi:10.5194/cp-3-423-2007, 2007.
- Ambach, W.: Heat balance characteristics and ice ablation, western EGIG-profile, Applied hydrology in the development of northern basins, Danish Society for Arctic Technology, Copenhagen, 1988.
- Bamber, J. L., Layberry, R. L., and Gogineni, S. P.: A new ice thickness and bed data set for the Greenland ice sheet; 1. measurement, data reduction, and errors, *J. Geophys. Res.*, 106, 33773–33780, 2001.
- Bintanja, R., van de Wal, R. S. W., and Oerlemans, J.: Global ice volume variations through the last glacial cycle simulated by a 3-D ice dynamical model, *Quatern. Int.*, 95–96, 11–23, 2002.
- Bonelli, S., Charbit, S., Kageyama, M., Woillez, M.-N., Ramstein, G., Dumas, C., and Quiquet, A.: Investigating the evolution of major Northern Hemisphere ice sheets during the last glacial-interglacial cycle, *Clim. Past*, 5, 329–345, doi:10.5194/cp-5-329-2009, 2009.
- Braithwaite, R. J.: Calculation of degree-days for glacier-climate research, *Zeitschrift für Gletscherkunde und Glazialgeologie*, 2°, 1–18, 1984.
- Braithwaite, R. J.: Positive degree-day factors for ablation on the Greenland ice sheet studies by energy-balance modelling, *J. Glaciol.*, 41, 153–160, 1995.
- Braithwaite, R. J. and Olesen, O. B.: Calculation of glacier ablation from air temperature, West Greenland, *Glacier fluctuations and climatic change*, Kluwer Academic Publisher, Dordrecht, 1989.
- Braithwaite, R. J. and Zhang, Y.: Sensitivity of mass balance of five Swiss glaciers to temperature changes assessed by tuning a degree-day model, *J. Glaciol.*, 46, 7–14, 2000.
- Brigham-Grette, J.: New perspectives on Berigian Quaternary paleogeography, stratigraphy and glacial history, *Quaternary Sci. Rev.*, 20, 15–24, 2001.
- Brun, E., Martin, E., Simon, V., Gendre, C., and Coléou, C.: An energy and mass model for snow cover suitable for operational avalanche forecasting, *J. Glaciol.*, 35, 333–342, 1989.
- Brun, E., David, P., Sudul, M., and Brunot, G.: A numerical snow model to simulate snow cover stratigraphy for operational avalanche forecasting, *J. Glaciol.*, 38, 13–22, 1992.
- Calov, R., Ganopolski, A., Claussen, M., Petoukhov, V., and Greve, R.: Transient simulation of the last glacial inception. Part I: glacial inception as bifurcation in the climate system, *Climate Dynam.*, 24, 545–561, 2005a.
- Calov, R., Ganopolski, A., Petoukhov, V., Claussen, M., Brovkin, V., and Kubatzki, C.: Transient simulation of the last glacial inception. Part II: sensitivity and feedback analysis, *Climate Dynam.*, 24, 563–576, 2005b.
- Charbit, S., Ritz, C., and Ramstein, G.: Simulations of Northern Hemisphere ice-sheet retreat: sensitivity to physical mechanisms involved during the Last Deglaciation., *Quaternary Sci. Rev.*, 21, 243–265, 2002.
- Charbit, S., Kageyama, M., Roche, D., Ritz, C. and Ramstein, G.: Investigating the mechanisms leading to the deglaciation of past northern hemisphere ice sheets with the CLIMBER-GREMLINS coupled model, *Global Planet. Change*, 48, 253–273, 2005.
- Charbit, S., Ritz, C., Philippon, G., Peyaud, V., and Kageyama, M.: Numerical reconstructions of the Northern Hemisphere ice sheets through the last glacial-interglacial cycle, *Clim. Past*, 3, 15–37, doi:10.5194/cp-3-15-2007, 2007.
- Claussen, M., Mysak, L. A., Weaver, A. J., Crucifix, M., Fichet, T., Loutre, M.-F., Weber, S. L., Alcamo, J., Alexeev, V. A., Berger, A., Calov, R., Ganopolski, A., Goosse, H., Lohman, G., Lunkeit, F., Mokhov, I. I., Petoukhov, V., Stone, P., and Wang, Z.:

- Earth system models of intermediate complexity: closing the gap in the spectrum of climate models, *Clim. Dynam.*, 18, 579–586, 2002.
- Dee, D.P., Uppala, S. M., Simmons, A. J., Berrisford, P., Poli, P., Kobayashi, S., Andrae, U., Balmaseda, M. A., Balsamo, G., Bauer, P., Bechtold, P., Beljaars, A. C. M., van de Berg, L., Bidlot, J., Bormann, N., Delsol, C., Dragani, R., Fuentes, M., Geer, A. J., Haimberger, L., Healy, S. B., Hersbach, H., Holm, E. V., Isaksen, I., Kallberg, P., Köhler, M., Matricardi, M., McNally, A. P., Monge-Sanz, B. M., Morcrette, J.-J., Park, B.-K., Peubey, C., de Rosnay, P., Tavolato, C., Thépaut, J.-N., and Vitart, F.: The ERA-Interim reanalysis: configuration and performance of the data assimilation system, *Quaternary Journal of Royal Meteorological Society*, 137, 553–597, doi:10.1002/qj.828, 2011.
- Ettema, J., van den Broeke, M. R., van Meijgaard, E., van de Berg, W. J., Bamber, J. L., Box, J. E., and Bales, R. C.: Higher surface mass balance of Greenland ice sheet revealed by high-resolution climate modelling, *Geophys. Res. Lett.*, 36, L12501, doi:10.1029/2009GLO38110, 2009.
- Fausto, R. S., Ahlstrom, A. P., van As, D., Johnsen, S. J., Langen, P. L., and Steffen, K.: Improving surface boundary conditions with focus on coupling snow densification and meltwater retention in large-scale ice-sheet models of Greenland, *J. Glaciol.*, 55, 869–878, 2009.
- Fettweis, X.: Reconstruction of the 1979–2006 Greenland ice sheet surface mass balance using the regional climate model MAR, *The Cryosphere*, 1, 21–40, doi:10.5194/tc-1-21-2007, 2007.
- Fettweis, X., Tedesco, M., van den Broeke, M., and Ettema, J.: Melting trends over the Greenland ice sheet (1958–2009) from spaceborne microwave data and regional climate models, *The Cryosphere*, 5, 359–375, doi:10.5194/tc-5-359-2011, 2011.
- Fettweis, X., Franco, B., Tedesco, M., van Angelen, J. H., Lenaerts, J. T. M., van den Broeke, M. R., and Gallée, H.: Estimating the Greenland ice sheet surface mass balance contribution to future sea level rise using the regional atmospheric climate model MAR, *The Cryosphere*, 7, 469–489, doi:10.5194/tc-7-469-2013, 2013.
- Finsterwalder, S. and Schunk, H.: Der Suldenferner, *Zeitschrift des Deutschen und Österreichischen Alpenvereins*, 18, 72–89, 1887.
- Fyke, J. G., Weaver, A. J., Pollard, D., Eby, M., Carter, L., and Mackintosh, A.: A new coupled ice sheet/climate model: description and sensitivity to model physics under Eemian, Last Glacial Maximum, late Holocene and modern climate conditions, *Geosci. Model Dev.*, 4, 117–136, doi:10.5194/gmd-4-117-2011, 2011.
- Gallée, H. and Duynkerke, P. G.: Air-snow interactions and the surface energy and mass balance over the melting zone of west Greenland during the Greenland Ice Margin Experiment, *J. Geophys. Res.*, 102, 13813–13824, 1997.
- Ganopolski, A., Calov, R., and Claussen, M.: Simulation of the last glacial cycle with a coupled climate ice-sheet model of intermediate complexity, *Clim. Past*, 6, 229–244, doi:10.5194/cp-6-229-2010, 2010.
- Graversen, R. G., Drijfhout, S., Hazeleger, W., van de Wal, R., Bintanja, R., and Helsen, M.: Greenland's contribution to global sea-level rise by the end of the 21st century, *Clim. Dynam.*, 37, 1427–1442, 2010.
- Greve, R.: On the response of Greenland ice sheet to greenhouse climate change, *Climatic Change*, 46, 289–303, 2000.
- Greve, R.: Relation of measured basal temperatures and the spatial distribution of the geothermal heat flux for the Greenland ice sheet, *Ann. Glaciol.*, 42, 424–432, 2005.
- Hock, R.: Temperature index melt modelling in mountain areas, *J. Hydrol.*, 282, 104–115, 2003.
- Huybrechts, P. and de Wolde, J.: The dynamic response of the Greenland and Antarctic ice sheets to multiple century climatic warming, *J. Climate*, 12, 2169–2188, 1999.
- Huybrechts, P., Letréguilly, A., and Reeh, N.: The Greenland ice sheet and greenhouse warming, *Palaeogeography, Paleoclimatology, Palaeoecology (Global and Planetary Change section)*, 89, 399–412, 1991.
- Janssens, Y. and Huybrechts, P.: The treatment of meltwater retention in mass-balance parametrizations of the Greenland ice sheet, *Ann. Glaciol.*, 31, 133–140, 2000.
- Kageyama, M., Charbit, S., Ritz, C., Khodri, M., and Ramstein, G.: Quantifying ice-sheet feedbacks during the last glacial inception, *Geophys. Res. Lett.*, 31, L24203, doi:10.1029/2004GLO21339, 2004.
- Key, J., Wang, X., Stroeve, J., and Fowler, C.: Estimating the cloudy sky albedo of sea ice and snow from space, *J. Geophys. Res.*, 106, 12489–12497, 2001.
- Lambeck, K. and Chappell, J.: Sea level change through the last glacial cycle, *Science*, 292, 679–686, 2001.
- Lambeck, K., Purcell, A., Funder, S., Kjaer, K. H., Larsen, E., and Möller, P.: Constraints on the Late Saalian to early Middle Weichselian ice sheet of Eurasia from field data and rebound modelling, *Boreas*, 35, 539–575, 2006.
- Laskar, J., Robutel, P., Joutel, F., Gastineau, M., Correia, A. C. M., and Levrard, B.: A long term numerical solution for the insolation quantities of the Earth, *Astron. Astrophys.*, 428, 261–285, 2004.
- Lefebvre, F., Gallée, H., van Ypersele, J. P., and Huybrechts, P.: Modelling of large-scale melt parameters with a regional climate model in South Greenland during the 1991 melt season, *Ann. Glaciol.*, 35, 391–397, 2002.
- Lefebvre, F., Fettweis, X., Gallée, H., van Ypersele, J.-P., Marbaix, P., Greuell, W., and Calanca, P.: Evaluation of a high resolution regional climate simulation over Greenland, *Clim. Dynam.*, 25, 99–116, doi:10.1007/s00382-005-0005-8, 2005.
- MacAyeal, D. R.: Large-scale ice flow over a viscous basal sediment: theory and application to ice stream B, Antarctica, *J. Geophys. Res.*, 94, 4071–4087, 1989.
- Oerlemans, J. and Hoogendoorn, N. C.: Mass-balance gradients and climatic changes, *J. Glaciol.*, 35, 399–405, 1989.
- Oerlemans, J. and Vugts, H. F.: A meteorological experiment in the melting zone of the Greenland ice sheet, *Bulletin of American Meteorological Society*, 74, 355–365, 1993.
- Peltier, W. R.: Global glacial isostasy and the surface of the ice-age Earth: the ICE-5G (VM2) model and GRACE, *Annual Reviews of Earth and Planetary Science*, 32, 111–149, 2004.
- Petit, J. R., Jouzel, J., Raynaud, D., Barkov, N. I., Barnola, J.-M., Basile, I., Bender, M., Chappelaz, J., Davis, M., Delaygue, G., Delmotte, M., Kotlyakov, V. M., Legrand, M., Lipenkov, V. Y., Lorius, C., Pépin, L., Ritz, C., Saltzman, E., and Stievenard, M.: Climate and atmospheric history of the past 420,000 years from the Vostok ice core, Antarctica, *Nature*, 399, 429–436, 1999.

- Petoukhov, V., Ganopolski, A., Brovkin, V., Claussen, M., Eliseev, A., Kubatzki, C., and Rahmstorf, S.: CLIMBER-2: a climate system model of intermediate complexity. Part I: model description and performance for present climate, *Clim. Dynam.*, 16, 1–17, 2000.
- Peyaud, V., Ritz, C., and Krinner, G.: Modelling the Early Weichselian Eurasian Ice Sheets: role of ice shelves and influence of ice-dammed lakes, *Clim. Past*, 3, 375–386, doi:10.5194/cp-3-375-2007, 2007.
- Pfeffer, W. T., Meier, M. F., and Illangasekare, T. H.: Retention of Greenland runoff by refreezing: implications for projected future sea level changes, *J. Geophys. Res.*, 96, 22117–22124, 1991.
- Philippon, G., Ramstein, G., Charbit, S., Kageyama, M., Ritz, C., and Dumas, C.: Evolution of the Antarctic ice sheet through the last deglaciation : a study with a new coupled climate-north and south hemisphere ice sheet model, *Earth Planet. Sc. Lett.*, 248, 750–758, 2006.
- Reeh, N.: Parameterization of melt rate and surface temperature on the Greenland ice sheet, *Polarforschung*, 59, 113–128, 1991.
- Reijmer, C. H., van den Broeke, M. R., Fettweis, X., Ettema, J., and Stap, L. B.: Refreezing on the Greenland ice sheet: a comparison of parameterisations, *The Cryosphere*, 6, 743–762, doi:10.5194/tc-6-743-2012, 2012.
- Ritz, C., Fabre, A., and Letréguilly, A.: Sensitivity of a Greenland ice sheet model to ice flow and ablation parameters: consequences for the evolution through the last climatic cycle, *Clim. Dynam.*, 13, 11–24, 1997.
- Ritz, C., Rommelaere, V., and Dumas, C.: Modeling the Antarctic ice sheet evolution of the last 420 000 years: implication for altitude changes in the Vostok region, *J. Geophys. Res.*, 106, 31943–31964, 2001.
- Robinson, A., Calov, R., and Ganopolski, A.: Greenland ice sheet model parameters constrained using simulations of the Eemian Interglacial, *Clim. Past*, 7, 381–396, doi:10.5194/cp-7-381-2011, 2011.
- Stone, E. J., Lunt, D. J., Rutt, I. C., and Hanna, E.: Investigating the sensitivity of numerical model simulations of the modern state of the Greenland ice-sheet and its future response to climate change, *The Cryosphere*, 4, 397–417, doi:10.5194/tc-4-397-2010, 2010.
- Svendsen, J. I., Alexanderson, H., Astakhov, V. I., Demidov, I., Dowdeswell, J., Funder, S., Gataullin, V., Henriksen, M., Hjort, C., Houmark-Nielsen, M., Hubberten, H. W., Ingolfsson, O., Jakobsson, M., Kjaer, K. H., Larsen, E., Lokrantz, H., Lunkka, J. P., Lysa, A., Mangerud, J., Matiouchkov, A., Murray, A., Möller, P., Niessen, F., Nikolskaya, O., Polyak, L., Saarnisto, M., Siegert, C., Siegert, M. J., Spielhagen, R. F., and Stein, R.: Late Quaternary ice sheet history of Northern Eurasia, *Quaternary Sci. Rev.*, 23, 1229–1271, 2004.
- Swingedouw, D., Fichet, T., Huybrechts, P., Goose, H., Driesschaert, E., and Loutre, M.-F.: Antarctic ice-sheet melting provides negative feedbacks on future climate warming, *Geophys. Res. Lett.*, 35, L17705, doi:10.1029/2008GLO34410, 2008.
- Tarasov, L. and Peltier, W. R.: Impact of thermomechanical ice sheet coupling of the 100 kyr ice age cycle, *J. Geophys. Res.*, 104, 9517–9545, 1999.
- Tarasov, L. and Peltier, W. R.: Greenland glacial history and local geodynamic consequences, *Geophys. J. Int.*, 150, 198–229, 2002.
- Tarasov, L., Dyke, A. S., Neal, R. M., and Peltier, W. R.: A data-calibrated distribution of deglacial chronologies for the North American ice complex from glaciological modelling, *Earth Planet. Sc. Lett.*, 315–316, 30–40, 2012.
- van den Broecke, M. R., Dyunkerke, P. G., and Oerlemans, J.: The observed katabatic flow at the edge of the Greenland ice sheet during GIMEX-91, *Global Planet. Change*, 9, 3–15, 1994.
- van den Broecke, M. R., Smeets, P., Ettema, J., and Munneke, P. K.: Surface radiation balance in the ablation zone of the west Greenland ice sheet, *J. Geophys. Res.*, 113, D13105, doi:10.1029/2007JD009283, 2008.
- Vizcaino, M., Mikolajewicz, U., Gröger, M., Maier-Reimer, E., Schurgers, G., and Winguth, A. M. E.: Long-term ice sheet-climate interactions under anthropogenic greenhouse forcing simulated with a complex Earth System Model, *Clim. Dynam.*, 31, 665–690, 2008.
- Waelbroeck, C., Labeyrie, L., Michel, E., Duplessy, J. C., McManus, J. F., Lambeck, K., Balbon, E., and Labracherie, M.: Sea-level and deep water temperature changes derived from benthic foraminifera isotopic records, *Quaternary Sci. Rev.*, 21, 295–305, 2002.
- Zweck, C. and Huybrechts, P.: Modeling of the northern hemisphere ice sheets during the last glacial cycle and glaciological sensitivity, *J. Geophys. Res.*, 110, D07103, doi:10.1029/2004JD005489, 2005.